Peer-reviewed version available at Polymers 2018, 10, 689; doi:10.3390/polym10060689

Article

Efficient Shielding of Polyplexes using Heterotelechelic Polysarcosines

Philipp Michael Klein [1,*], Kristina Klinker [2,4], Wei Zhang [1], Sarah Kern [1], Eva Kessel [1], Ernst Wagner [1,3], Matthias Barz [2,*]

[1] Ludwig-Maximilians-Universität (LMU) Munich, Pharmaceutical Biotechnology, Department of Pharmacy, Butenandtstrasse 5-13, D-81377 Munich, Germany; philipp.klein@cup.uni-muenchen.de
[2] Institute of Organic Chemistry, Johannes Gutenberg University, Duesbergweg 10-14, D-55128 Mainz, Germany Affiliation 2; barz@uni-mainz.de
[3] Nanosystems Initiative Munich, Schellingstraße 4, D-80799 Munich, Germany
[4] Graduate School Materials Science in Mainz, Staudinger Weg 9, 55128 Mainz, Germany

* Correspondences: philipp.klein@cup.uni-muenchen.de; Tel.: +49-89-2180-77794
barz@uni-mainz.de; Tel.: +49-6131-39-26256

Abstract: Shielding agents are commonly used to shield polyelectrolyte complexes, e.g. polyplexes, from agglomeration, precipitation in complex media, like blood, and thus enhance their circulation times in vivo. Since up to now primarily poly(ethylene glycol) (PEG) has been investigated to shield non-viral carriers for systemic delivery, we report on the use of polysarcosine (pSar) as a potential alternative for steric stabilization. A redox-sensitive, cationizable lipo-oligomer structure (containing two cholanic acids attached via a bioreducible disulfide linker to an oligoaminoamide backbone in T-shape configuration) was equipped with azide-functionality by solid phase supported synthesis. After mixing with small interfering RNA (siRNA), lipopolyplexes formed spontaneously and were further surface-functionalized with polysarcosines. Polysarcosine was synthesized by living controlled ring-opening polymerization using an azide-reactive dibenzo-aza-cyclooctyne-amine as an initiator. The shielding ability of the resulting formulations was investigated with biophysical assays and by near-infrared fluorescence bioimaging in mice. The modification of ~100 nm lipopolyplexes was only slightly increased upon functionalization. Cellular uptake into cells was strongly reduced by the pSar shielding. Moreover, polysarcosine-shielded polyplexes showed enhanced blood circulation times in bioimaging studies compared to unshielded polyplexes and similar to PEG-shielded polyplexes. Therefore, polysarcosine is a promising alternative for the shielding of non-viral, lipo-cationic polyplexes.

Keywords: shielding agent, polysarcosine, biodistribution, click-chemistry, lipopolyplex, nucleic acid carrier

1. Introduction

Therapeutic nucleic acids are powerful tools, which can be used to specifically control gene expression inside cells [1-5]. For several diseases, including severe metastatic tumors, systemic delivery is required to achieve therapeutic effect. Naked oligonucleotides have limited stability in biological fluids because they are actively targeted and degraded by nucleases. Although this issue might be addressed by the incorporation of chemical modifications [6,7], the renal clearance of small oligonucleotides or siRNA usually occurs within a few minutes, which limits the time to reach their desired site of action [8,9]. Liposome-based formulations, lipo-polymer micelles, and polymer-based complexes increase the size usually beyond the renal cut-off and thus enhance circulation times, whenever a stealth-like corona protects the systems from unspecific aggregation [6,10-21]. Various

polycations, cationic lipids and combinations with helper lipids are used to form polyplexes [4,14,16,17,22-24], lipoplexes or lipid nanoparticles (LNPs) [1,11,25-30]. Precise editing of the components' chemical structure enables the fine-tuning of a carrier's stability and size, but also other properties, which are important for the delivery process like cellular uptake, endosomal escape ability, and cell tolerability [31-34].

Solid phase-supported synthesis (SPS) is a very convenient and precise way to optimize a delivery system in a step-wise manner [18,35]. Recently, we developed our own customized amino acids, such as succinoyl tetraethylene pentamine (Stp), which contains of short defined repeats of the diaminoethane motif prepared in boc/fmoc protected form. With artificial building blocks, natural α-amino acids and fatty acids we sequentially synthesized monodisperse cationic oligomers via SPS, which are highly adaptable to different demands in the field of gene delivery [8,12,18,31-33,36-39]. By precise incorporation of a bioreducible cleavage site between the cationic and a lipophilic block, for instance, it was possible to destabilize polyplexes only after reaching the cytoplasm of the cell [39]. Thereby the carrier system remained stable in serum and transfection efficiency as well as cell viability could be increased in certain cell lines.

Besides size and stability, the surface character of a nanoparticle is of utmost importance for its systemic delivery. Shielding agents attached to the surface prevent interactions with neighboring particles and/or blood components, which usually leads to extended circulation in the body's bloodstream [40-42]. Already in 1990 it could be demonstrated that polyethylene glycol (PEG) could extend the blood circulation half-life of systemically administered liposomes from <30 min to several hours [40]. Its hydrophilic character enables PEG to generate a hydrated shell covering the nanoparticles and thereby sterically reduce unwanted interactions with biomolecules or other poly- or lipoplexes [43]. PEG is the most prominent shielding agent and has often been used to shield cationic polyplexes in numerous applications [44-49]. A major drawback, however, is that more and more researchers in academia or industry observe immune responses towards PEGylated nanoparticles [43,50-55]. For this reason several new alternatives were evaluated for shielding, such as natural proteins [56], oligosaccharides [57,58], poly(*N*-(2-hydroxypropyl)methacrylamide) (pHPMA) [58-60], hydroxyethyl starch (HES) [61] or polypeptides (poly(glutamic acid) [62], poly(hydroxyethyl-L-asparagine) [63], poly(hydroxyethyl-L-glutamine) [63], prolin-alanin-serin motif (PAS) [64,65]). Nevertheless, according to the Whiteside's rules for protein resistant surfaces an ideal alternative to PEG should mimic its chemical properties, being a hydrophilic, non-charged polymer and a weak hydrogen acceptor without donor properties, which is not the case for all above-mentioned polymers. In contrast, polysarcosine fulfills all the described criteria and has already demonstrated protein resistant properties on various surfaces [66-68]. In addition, it can be also synthesized by living controlled ring opening polymerization of the corresponding *N*-carboxyanhydrides (NCA) [69,70]. However, *in vivo* data on polysarcosine is rarely reported in literature [71]. In contrast to polypeptides, the side chain of polypeptoids is situated at the nitrogen rather than the α-carbon, in the case of pSar the nitrogen is methylated. As a result, polysarcosine adopts a random coil conformation in aqueous solution and possesses a comparable second virial coefficient and molecular weight dependency like PEG [72]. All these properties provide a high resistance against protein adsorption [73] and make it in theory an ideal material for shielding electrostatic complexes *in vivo* [74]. Importantly, it has been reported that polysarcosine has so far demonstrated neglectable complement activation or immunogenicity in mouse, rat and rabbit animal models [75,76]. And pSar-shielded polyplexes, micelles, colloids and nanohydrogels demonstrated the absence of aggregation in human serum [77-80].

In the current work, we have incorporated azide domains into a previously described redox-sensitive T-shaped bis-(cholanic acid amido) oligoaminoamide siRNA carrier system [39] and used strain-promoted azide-alkyne cycloaddition (SPAAC) reaction to equip the surface of lipopolyplexes with ~8 kDa polysarcosine (DP=119) chains. We report on the ability of polysarcosine to shield siRNA lipoplexes and analyzed the *in vivo* stability and biodistribution after intravenous administration into mice. In a second approach, we modified the system with a folate ligand to target the folate receptor overexpressed on certain cancer cells [81-86].

2. Materials and Methods

2.1 Materials

Protected Fmoc-α-amino acids, 2-chlorotrityl chloride resin, *N*,*N*-dimethylformamide (DMF), *N*,*N*-diisopropylethylamine (DIPEA) and trifluoroacetic acid (TFA) for solid-phase syntheses were purchased from Iris Biotech (Marktredewitz, Germany). Triisopropylsilane (TIS), 1-hydroxybenzotriazole (HOBt), 5β cholanic acid. Dimethylformamide (DMF) for DBCO-PSar syntheses was purchased from Acros Organics (99.8% Extra), further dried over CaH2 and fractionally distilled *in vacuo*. Folic acid (FolA) was purchased from Acros Organics (96–102% pure). Triethylamine (TEA) and *N*,*N*-diisopropylethylamine (DIPEA) were dried over NaOH and fractionally distilled *in vacuo*. (Benzotriazol-1-yloxy) tripyrrolidino phosphonium hexafluorophosphate (PyBOP), 2-(1H-Benzotriazol-1-yl)-1,1,3,3-tetramethyluronium-hexafluorphosphat (HBTU) and microreactors were obtained from MultiSynTech (Witten, Germany). Cell culture media, antibiotics and fetal calf serum (FCS) were purchased from Invitrogen (Karlsruhe, Germany), HEPES from Biomol GmbH (Hamburg, Germany), glucose from Merck (Darmstadt, Germany), agarose (NEEO Ultra-quality) from Carl Roth GmbH (Karlsruhe, Germany), and GelRed™ from VWR (Darmstadt, Germany). Cell culture 5 × lysis buffer and D-luciferin sodium salt were obtained from Promega (Mannheim, Germany). Ready-to-use siRNA duplexes were obtained from Axolabs GmbH (Kulmbach, Germany): eGFP-targeting siRNA (siGFP) (sense: 5′-AuAucAuGGccGAcAAGcAdTsdT-3′; antisense: 5′-UGCUUGUCGGCcAUGAuAUdTsdT-3′) for silencing of eGFPLuc; control siRNA (siCtrl) (sense: 5′-AuGuAuuGGccuGuAuuAGdTsdT-3′; antisense: 5′-CuAAuAcAGGCcAAuAcAUdTsdT-3′); Cy5-labled siRNA (Cy5-siAHA1) (sense: 5′-(Cy5)(NHC6)GGAuGAAGuGGAGAuuAGudTsdT-3′; antisense: 5′-ACuAAUCUCcACUUcAUCCdTsdT-3′); Cy7-labled siRNA (Cy7-siAHA1) (sense: 5′-(Cy7)(NHC6)GGAuGAAGuGGAGAuuAGudTsdT-3′; antisense: 5′-ACuAAUCUCcACUUcAUCCdTsdT-3′) small letters: 2′methoxy; s: phosphorothioate. All other chemicals were purchased from Sigma (Munich, Germany), Iris Biotech (Marktredwitz, Germany), Merck (Darmstadt, Germany) or AppliChem (Darmstadt, Germany), Acros Organics, Alfa Aesar, or Fluka.

2.2 Synthesis of oligomers and DBCO shielding agents

2.2.1 Synthesis of oligomers

See supporting information for detailed description on syntheses of oligomers.

2.2.2 Synthesis of sarcosine-*N*-carboxyanhydride

The synthesis was performed as described in Klinker et al. [71] Sarcosine (15.16 g, 170.2 mmol, 1 eq) was weighed into a pre-dried three-necked flask and dried under vacuum for 1 hour. 300 mL absolute (abs) THF was added under a steady flow of nitrogen. The apparatus was connected to two gas washing bottles filled with aqueous sodium hydroxide solution. Diphosgene (16.26 ml, 134 mmol, 0.8 eq) was added slowly via syringe. The colorless suspension was heated to 70 °C yielding a clear solution after 3 hours of stirring. The solvent was evaporated under reduced pressure yielding a brown oil as crude reaction product. The oil was heated to 50 °C and dried under reduced pressure to obtain an amorphous solid. The crude reaction product was redissolved in 60 mL THF and precipitated with 300 mL abs n-hexane. The precipitate was filtered off under N_2-atmosphere and dried with a stream of dry nitrogen for 60 - 90 minutes to remove residual traces of solvents. The next day, the product was dried in high vacuum for 2 hours in the sublimation apparatus and subsequently sublimated at 80 – 85 °C and < $1x10^{-2}$ mbar. The product was collected from the sublimation apparatus in a glove box on the same day. Colorless crystals were obtained (50 – 67 %). mp = 104.3 °C; ^{1}H NMR (300 MHz, $CDCl_3$) δ[ppm] = 2.86 (s, 3H, NH-CH_3), 4.22 (s, 2H, NH-CH_2-CO).

2.2.3 Synthesis of DBCO-PSar

DBCO-PSar was synthesized using ring-opening polymerization of SarNCA as described in Klinker et al. [71] In a typical experiment, 461.8 mg of SarNCA (4.012 mmol) were transferred under nitrogen counter flow into a pre-dried Schlenk-tube, equipped with a stir bar and again dried in vacuum for 30 minutes. The NCA was then dissolved in 3.5 ml of dry DMF. A stock solution of DBCO-amine (0.074 mmol, 1/110 eq, M/I = 110) in 2 mL DMF was prepared and 1 mL of this stock solution were added to the monomer solution via syringe. The solution was stirred at 40 °C and kept at a constant pressure of 1.25 bar of dry nitrogen via the Schlenk-line to prevent impurities from entering the reaction vessel while allowing CO_2 to escape. Completion of the reaction was confirmed by IR spectroscopy (disappearance of the NCA peaks (1853 and 1786 cm^{-1})). Directly after completion of the reaction, the polymer was precipitated in cold diethyl ether and centrifuged (4500 rpm at 4 °C for 15 min). After discarding the liquid fraction, new ether was added and the polymer was resuspended using sonication. The suspension was centrifuged again and the procedure was repeated. The polymer was then dissolved in H_2O and lyophilized to obtain a fluffy powder (279.7 mg, 98 %). ^{1}H-NMR: (400 MHz, DMSO–d_6): δ [ppm] = 0.88 – 0.79 (m, ini, 9H, -C(CH_3)$_3$), 2.58 - 3.11 (br, 3nH, N-CH_3), 3.73 - 4.57 (br, 2nH, -CO-CH_2-N), = 7.86 – 7.10 (m, 8H, benzylic protons).

2.2.4 Synthesis of DBCO-PSar-Ac

DBCO-PSar119 (Mn =8735 g mol^{-1}) (36 mg, 0.004 mmol), acetic anhydride (4.2 mg, 3.9 µL, 0.04 mmol), and triethylamine (10.7 mg, 14.6 µL, 0.08 mmol) were dissolved in absolute DMF (1 mL) and stirred at 25 °C for 24 h under an argon atmosphere. Subsequently, the polymer was precipitated in diethyl ether, extensively dialyzed against water (MWCO = 3500 g mol^{-1}), and lyophilized. Yield after dialysis: 25 mg (69%).

2.2.5 Synthesis of DBCO-PSar-FolA

DBCO-PSar$_{110}$ (Mn =8095 g mol^{-1}) (55.8 mg, 0.007 mmol) was separately dissolved in absolute DMSO. Folic acid (30.4 mg, 0.068 mmol), HBTU (26.1 mg, 0.068 mmol), and HOBt (9.31 mg, 0.068 mmol) were dissolved in DMSO and cooled to 0 °C. DIPEA (17.8,mg, 24.0 µL, 0.138 mmol) was added and the mixture was left to react for 30 minutes at 0 °C. The in situ formed activated ester was added to the predissolved polymer and the reaction mixture was stirred at 25 °C for 24 h under an argon atmosphere. The crude reaction product was purified by size exclusion chromatography in DMSO using a Sephadex LH-20-packed column. The purified conjugate was lyophilized from water. Yield after SEC: 31 mg (55%).

2.2.6 Gel permeation chromatography

Polymer molecular weight and dispersity index were determined by gel permeation chromatography (GPC). GPC in hexafluoro-2-propanol (HFIP) was performed with 3 g L^{-1} potassium trifluoroacetate (KTFA) at 40 °C. The columns were packed with modified silica (PFG columns, particle size: 7 µm; porosity: 100 and 1000 Å). A refractive index detector (G 1362A RID, Jasco) and a UV/vis detector (UV-2075 Plus, JASCO, λ=230 nm; λ=330nm for folic acid detection) were used to detect the polymer. Molecular weights were calculated using calibration performed with PMMA standards (Polymer Standards Services GmbH). Toluene was used as the internal standard.

2.2.7 UV-vis spectroscopy

UV-vis absorbance spectra were recorded using a spectrophotometer V-630 (Jasco) with water being the solvent.

192 *2.3 Formation of siRNA polyplexes*

193 siRNA was dissolved in 20 mM HEPES buffered 5% glucose pH 7.4 (HBG) at a concentration of
194 50 ng/µL for *in vitro* experiments and 500 ng/µL for *in vivo* experiments. According to the indicated
195 nitrogen/phosphate (N/P) ratio, the oligomer solution was prepared in a separate tube. Only
196 protonatable nitrogens were considered in the N/P calculation. The same volume of siRNA solution
197 was added to the oligomer. The mixture was rapidly pipetted at least five times and incubated for
198 40 min at RT resulting in a polyplex solution with 25 or 250 ng of siRNA/µL respectively.

199 *2.4 Functionalization of polyplexes with DBCO reagents*

200 For functionalization of siRNA polyplexes with DBCO click agents, solutions with reagents were
201 prepared in ¼ of the volume of polyplex solutions prepared before. The concentration of the solution
202 was calculated according to the respective equivalents (eq). Equivalents represent the molar ratio of
203 shielding agent to oligomer in the polyplex solution. The reaction time was 16 h for biophysical and
204 *in vitro* assays and 4 h for *in vivo* experiment respectively.

205 *2.5 siRNA binding assays*

206 siRNA binding assays were performed analogously as described in Klein et al. [86]. A 1%
207 agarose gel was prepared by dissolving agarose in TBE buffer (10.8 g of trizma base, 5.5 g of boric
208 acid, 0.75 g of disodium EDTA, and 1 L of water) and subsequent boiling. After cooling down to
209 about 50 °C, GelRed™ was added. Formulations were prepared with 50 ng of siRNA. Samples were
210 placed into the pockets after 4 µl of loading buffer (prepared from 6 mL of glycerine, 1.2 mL of 0.5 M
211 EDTA, 2.8 mL of H_2O, 0.02 g of bromophenol blue) was added. Electrophoresis was performed at
212 70 V for 60 min.

213 *2.6 Particle size and zeta potential measurements*

214 Dynamic light scattering (DLS) measurements of polyplex solutions were performed in a folded
215 capillary cell (DTS 1070) using a Zetasizer Nano ZS with backscatter detection (Malvern Instruments,
216 Worcestershire, UK). Polyplexes were formed using 2 µg siRNA in a total volume of 80 µL. For size
217 measurements, the equilibration time was 0 min, the temperature was 25 °C and an automatic
218 attenuator was used. The refractive index of the solvent was 1.330 and the viscosity was 0.8872 mPa·s.
219 Each sample was measured 3 times. For detection of the zeta potential, the sample was diluted to
220 800 µL volume with 10 mM NaCl solution. Measurements with at least 6 runs were performed. Zeta
221 potentials were calculated by the Smoluchowski equation. Ten to fifteen sub runs lasting 10 s each at
222 25 °C (n = 3) were measured.

223 *2.7 Cell culture*

224 The mouse neuroblastoma cells (Neuro2a) were cultured in DMEM low glucose medium
225 (Sigma, Munich, Germany). As FR-expressing cell lines, human cervix carcinoma cells (KB), and
226 human cervix carcinoma cells stably transfected with the eGFPLuc (enhanced green fluorescent
227 protein/luciferase) gene (KB/eGFPLuc) were cultured in folate-free RPMI 1640 medium (Invitrogen,
228 Karlsruhe, Germany). All media were supplemented with 10% FBS, 100 U/mL penicillin, and 100
229 µg/mL streptomycin. The cells were maintained in ventilated flasks in the cell incubator at 37 °C with
230 5% CO_2 in a humidified atmosphere. Cell lines were grown to 80-90% confluency and harvested.

231 *2.8 Cell association and internalization of siRNA polyplexes measured with flow cytometry*

232 For untargeted polyplexes, Neuro2a cells were seeded in 24-well plates with 5×10^4 cells/well at
233 24 h before the experiment, and fresh growth medium was provided before the experiment.
234 Polyplexes containing 1.5 µg of siRNA (including 20% Cy5-labeled siRNA) were added into each
235 well incubated for four hours at 37 °C in 5% CO_2. Cells were then incubated with 500 I.U. heparin to
236 remove polyplexes non-specifically associated to the cell surface.

For folate-targeted polyplexes, KB cells were seeded in 24-well plates with 5 × 10^4 cells/well at 24 h before the experiment, and fresh growth medium was provided before the experiment. Polyplexes containing 1.5 µg of siRNA (including 20% Cy5-labeled siRNA) were added into each well incubated 30 min on ice for cell association or 45 min at 37 °C in 5% CO_2 for cellular internalization, respectively. Cells were washed with PBS to remove free polyplexes. For cellular internalization, cells were then incubated with 500 I.U. heparin to remove polyplexes non-specifically associated to the cell surface.

Finally, cells were collected and resuspended in PBS buffer with 10% FBS. All samples were measured by flow cytometry with CyanTM ADP (Dako, Hamburg, Germany) through excitation at 635 nm, and detection of emission at 665 nm. Dead cells were differentiated by DAPI fluorescence and removed by gating in order to analyze cellular uptake of polyplexes in living cells. Data were analyzed by FlowJo 7.6.5 flow cytometric analysis software.

2.9 Confocal laser scanning microscopy (CLSM)

Neuro2a cells were seeded into an 8-well Lab-Tek chamber slide (Nunc) at a density of 3 × 10^4 cells/well in 300 µL of growth medium 24 h prior to treatment. Polyplexes were formed as described using a 1.5µg of a mixture of 80% of siCtrl and 20% Cy5-labeled siRNA and oligomer at N/P 12 in 60 µL of HBG followed by the indicated agent in 20µL. Cells were incubated with 220 µL of fresh growth medium and polyplex solution was applied. For the uptake study, the incubation with polyplexes was at 37 °C for 4 h. The growth medium was removed, cells were washed twice with 300 µL of PBS and fixed with 4% PFA solution for 30 min at room temperature. Cell nuclei were stained with DAPI. A Leica TCS SP8 confocal microscope was used for image acquisition.

2.10 Mouse tumor model

Female six- to seven-week-old nude mice, Rj: NMRI-nu (nu/nu) (Janvier, Le Genest-Saint-Isle, France), were housed in isolated ventilated cages under specific pathogen-free condition with a 12 h light/dark interval and were acclimated for at least 7 days prior to experiments. Food and water were provided *ad libitum*. Animals were injected subcutaneously with 5 × 10^6 Neuro2a cells. The body weight was recorded, and the tumor volume was measured by caliper and calculated as [0.5 × (longest diameter) × (shortest diameter)^2]. All animal experiments were performed according to guidelines of the German Animal Welfare Act and were approved by the local animal ethics committee.

2.11 Biodistribution study

For near infrared (NIR) *in vivo* imaging, unlabeled control siRNA (siCtrl) was spiked with 50% of Cy7-labeled siRNA (Cy7-siAHA1) in HBG. When tumors reached the size of 500 - 1000 mm^3, the mice (n = 2/per group) were anesthetized with 3% isoflurane in oxygen. siRNA polyplexes containing 50 µg of Cy7-labeled siRNA (N/P 10) in 250 µL (containing 100 µL of siRNA solution, 100 µL of oligomer solution, 50 µL of agent solution or buffer) of HBG were injected intravenously (i.v.), and fluorescence was measured with a CCD camera at different time points. For evaluation of images, the efficiency of fluorescence signals was analyzed after color bar scales were equalized using the IVIS Lumina system with Living Image software 3.2 (Caliper Life Sciences, Hopkinton, MA, USA).

3. Results and Discussion

3.1 Design and synthesis of a lipo-oligomer for click chemistry

In previous work, we have established a new class of redox-sensitive lipo-oligomers prepared by solid-phase supported synthesis (SPSS) to serve as carriers for siRNA delivery [39]. Beside beneficial effects of lipid-based delivery systems, such as enhanced nanoparticle stability and endosomal escape capability, the *in vivo* distribution is often limited to certain tissues, primarily liver, lung and spleen [87-89]. In previous studies, it has been shown that T-shape oligomers similar to the

Preprints (www.preprints.org) | NOT PEER-REVIEWED | Posted: 29 May 2018 doi:10.20944/preprints201805.0423.v1

Peer-reviewed version available at Polymers 2018, 10, 689; doi:10.3390/polym10060689

ones that were synthesized in this approach demonstrate the strongest retention in liver tissue [89,90]. Those effects might be related to a high stickiness of cationic particles, but it is also possible that certain serum proteins, which incorporate onto nanoparticle surfaces may impair tissue specificity [88,91-93]. An efficient shielding should reduce both types of interactions and should enable a better distribution in the body. For this reason, one of the best performing candidates from redox-sensitive lipo-oligomers, T-shape structure ***T-0N3*** (published as ID ***992*** in [39]) was chosen and extended by click-reactive azide functionality. After the formation of siRNA lipopolyplexes, the particle surface was further modified with the shielding agents.

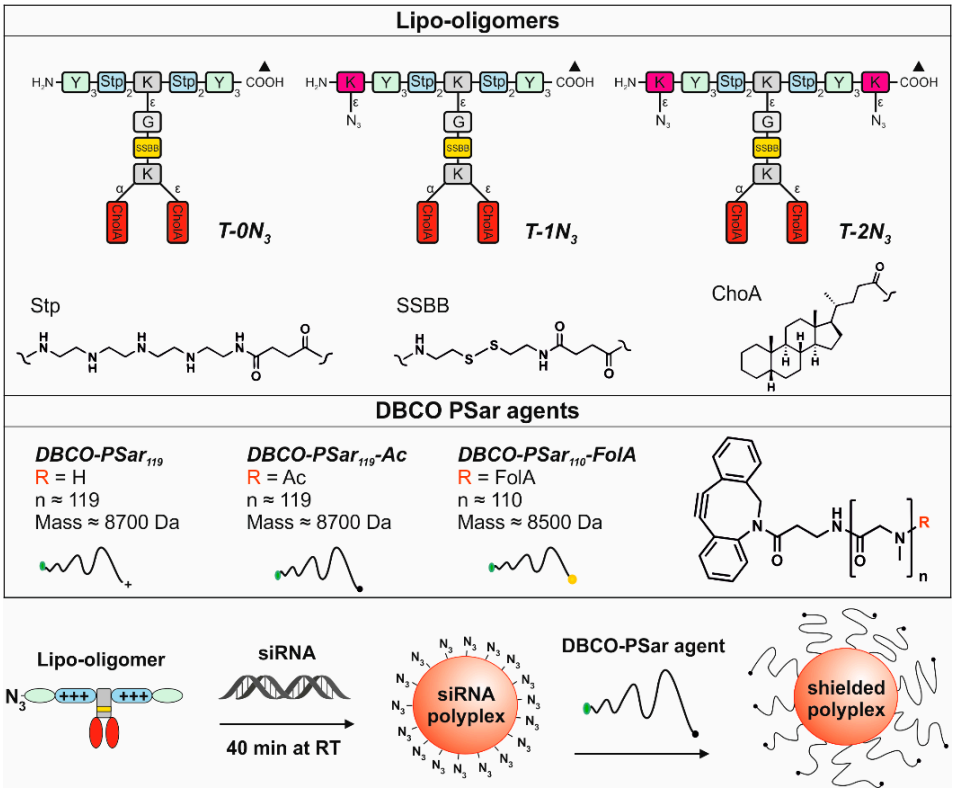

Figure 1. Overview of chemical compounds. Table, top: schematic illustration of sequence-defined oligomers with T-shape topology; ***T-0N3*** (ID: ***992*** published [39]), ***T-1N3*** (ID: ***1073***) and ***T-2N3*** (ID: ***1086***) with no, one or two terminal azidolysines K(N3). Other units of the oligomers: Y: tyrosine, K: lysine, G: glycine, Stp: succinoyl-tetraethylene-pentamine, ssbb: succinoyl-cystamine, CholA: 5β-Cholanic acid. The broken lines represent amide linkages, the triangle (▲) is the starting point of the synthesis. IDs are unique database identification numbers. Table, bottom: structure of the shielding agents ***DBCO-PSar119***, ***DBCO-PSar119-Ac*** and ***DBCO-PSar110-FolA***. Scheme of the formulation of a shielded polyplex.

T-0N3 was chosen as starting point for further modifications, because it forms stable siRNA polyplexes with sizes below 200 nm hydrodynamic diameter, which show high transfection efficiency in mouse neuroblastoma (Neuro2a) cells. This structure combines natural amino acids and artificial building blocks (Figure 1 - top). It consists of four repeats of the cationic polyamino acid succinoyl-tetraethylene-pentamine (Stp) used for complexation of nucleic acid and for endosomal buffering. Two tyrosine trimer units flanking the cationic domain stabilize the polyplex due to their hydrophobicity and π–π stacking ability. In the center of the cationic Stp units, two hydrophobic cholanic acids branch off the cationic backbone (T-shape) for lipopolyplex stabilization. The lipid and cationic domains are connected via a bioreducible linking unit (ssbb) [39]. In this approach, the azide function was incorporated into the oligomer during standard Fmoc solid-supported synthesis via an azidolysine residue at the N- and/or C-terminus of the backbone (structures ***T-1N3*** with one azide and ***T-2N3*** with two azides, Figure 1 - top). Consequently, the structure can be subsequently further modified with an alkyne-bearing functional group via click chemistry.

3.2 Synthesis of DBCO-modified polysarcosine

Polysarcosine is a hydrophilic, nonionic peptoidic structure with exclusively weak hydrogen bond acceptor properties. As shown empirically by Whitesides and co-workers for protein-resistant surfaces, these properties are essential to achieve "stealth"-like properties in a material [71,74]. Polysarcosine can be functionalized at its *N*-terminal (via post-polymerization modification) and *C*-terminal (via functional initiators) end. It is conveniently synthesized by controlled living ring-opening polymerization of α-amino acid *N*-carboxyanhydrides (NCA) with low dispersity index ($Đ_{GPC} \leq 1.1$; see **Table S1**) [71]. Initiating the reaction with dibenzo-aza-cyclooctyne-amine (DBCO-amine) leads to a C-terminal DBCO end group (Figure S1A) [94]. To ensure end group accessibility and steric stabilization at once we aimed for a degree of polymerization of around 115, which correlates with the PEG5k used as reference material. Therefore, a theoretical degree of polymerization of 115 was set by the monomer to initiator ratio. The polymerization was carried out under the conditions recently reported by Klinker et al. [95], NMR end group and SEC analysis (using pSar standards as described by Weber et al. [72]) revealed a number average degree of polymerization (DP) of 119 and a weight average DP of 8735 g mol^{-1} (Table S1), which is within the experimental error. The accuracy molecular weight determination is perfectly in line with the calculated one. The synthesized polymer displays a symmetrical SEC elugram indicating a Poisson-like molecular weight distribution, as expected for the amine initiated NNCA polymerization. The terminal DBCO can be clearly detected in the ^{1}H-NMR spectra and thus can be employed for the strain promoted azide-alkyne cycloadditon (SPAAC) with azides. For SPAAC no catalyst is needed, no side reactions with other functional domains of the oligomer can occur, and no toxic by-products are generated [96]. Mixing azide-modified cationic oligomers with siRNA leads to spontaneous assembly of polyplexes. Due to oligomer excess, several azide functionalities are accessible on the polyplex surface and can serve as attachment points for functionalization with DBCO-modified pSar. The *N*-terminal free amine group can further be modified with carboxylic acid-bearing molecules to introduce a second functionality, e.g. targeting ligands such as folic acid or alternatively may be capped by acetylation to remove the terminal amine, which is positively charged in aqueous solution of neutral pH. All synthesized agents are presented in Figure 1.

3.3 Polyplex formation and pSar-shielding

For polyplex formation, the structures ***T-1N$_3$*** and ***T-2N$_3$*** were incubated with siRNA for 40 min with a final concentration of 25 ng siRNA/µL. The electrophoretic mobility of incorporated siRNA was measured with an agarose gel shift assay to test the oligomers' abilities to bind nucleic acid. Different N/P values depict the ratio of amines (N) of the oligomers that can be protonated to the phosphates (P) of the siRNA. Like its azide-free analogue ***T-0N$_3$*** [39], the oligomers showed complete retention of siRNA in the pockets of the gel at an N/P ratio of 12 (Figure S2). No changes in binding ability were observed for the incorporation of one or two azides.

Next, the heterotelechelic polysarcosine with DBCO-end group (***DBCO-PSar$_{119}$***; Figure 1, bottom) was used to react with the azides on the preformed polyplexes (N/P ratio 12) to introduce a shielding layer. The SPAAC was allowed to proceed until full conversion for 16 hours (see scheme in Figure 1, bottom).

Afterwards, the influence of the pSar shielding agent on electrophoretic mobility was evaluated with respect to the number of azide functions incorporated into the polyplex-forming core structures (N_3 = 0, 1, 2). The amount of ***DBCO-PSar$_{119}$*** added to the polyplexes was kept constant (Figure 2A). In this experiment, only the azide-bearing polyplexes migrated in the gel towards the cathode, whereas the azide-free polyplex remained in the loading pocket. This demonstrates that a covalent bond connecting the shielding agent to the nanoparticle is crucial to provide this migratory effect. The migration of the integrated siRNA against its own negative charge shows that it is fully shielded against the force of the electric field. With increasing equivalents of ***DBCO-PSar$_{119}$***, stronger migration could be observed. This effect can be explained by the degree of polyplex surface modification (Figure 2B). For the oligomer with only one azide functionality (***T-1N$_3$***), maximum migration was achieved with equimolar amounts of DBCO click agent (1 eq / oligomer). More ***DBCO-***

Preprints (www.preprints.org) | NOT PEER-REVIEWED | Posted: 29 May 2018 doi:10.20944/preprints201805.0423.v1

Peer-reviewed version available at Polymers 2018, 10, 689; doi:10.3390/polym10060689

***PSar*$_{119}$** (2 eq) did not increase the effect. ***T-2N*$_3$** siRNA polyplexes with two azide functionalities within the carrier also showed the maximum migration for equimolar ratios of azide to DBCO (2 eq ***DBCO-PSar*$_{119}$**). These findings are in line with covalent modification with PEG5k [86].

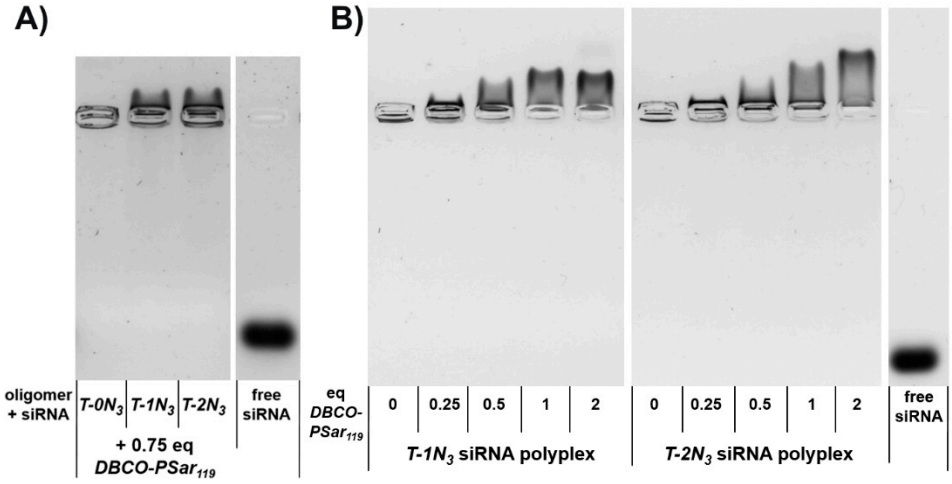

Figure 2. Electrophoretic mobility of siRNA polyplex formulations analyzed with an agarose gel shift assay A) siRNA polyplexes formed with oligomers bearing no (***T-0N*$_3$**), one (***T-1N*$_3$**) and two (***T-2N*$_3$**) azide functions incubated with 0.75 equivalents of ***DBCO-PSar*$_{119}$** 1 % agarose gel, 70 V, 80 min runtime. B) Formulations with increasing equivalents (eq mol/mol) of ***DBCO-PSar*$_{119}$**. 0.75 % agarose gel, 100V, 80 min runtime. All polyplexes were incubated for 40 min at N/P 12, followed by ***DBCO-PSar*$_{119}$** addition for 16 h at room temperature. The right lane shows the running distance of free siRNA not complexed by lipo-oligomers.

A second indirect measure for the efficiency of polyplex shielding is the zeta potential or electrochemical mobility. The latter can be determined by measuring a particle's mobility in an electric field with light scattering. In this respect, we observed that the positive zeta potential of an unshielded particle can be strongly reduced from 21 mV to 6 mV in case of ***T-1N*$_3$** polyplexes and from 17 mV to 3 mV in case of ***T-2N*$_3$** polyplexes, when the particle is shielded with an excess of ***DBCO-PSar*$_{119}$** (Table 1). By using 0.5 eq ***DBCO-PSar*$_{119}$** / oligomer, the zeta potential can already be reduced to 50%. It should be noted here that due to the *N*-terminal cationic tail group, the zeta potential always remained slightly positive.

As determined by single-angle dynamic light scattering (DLS), hydrodynamic diameters of the polyplexes were approximately 100 nm. With increasing amounts of ***DBCO-PSar*$_{119}$**, the nanoparticle size increased by up to 16 nm in diameter. pSar covering the particle surface seems to be the most plausible explanation for the increase in size.

Table 1. Particle size (z-average) and zeta potential of pSar-shielded siRNA formulations determined by a dynamic light scattering (DLS) zetasizer. siRNA polyplexes were prepared at N/P 12

siRNA formulation	eq DBCO-PSar$_{119}$	z-average [nm]	PDI	Mean Zeta Potential [mV]
***T-1N*$_3$**	0	81.0 ± 5.0	0.26 ± 0.02	20.9 ± 0.9
	0.5	86.7 ± 2.8	0.24 ± 0.02	9.4 ± 0.5
	1	91.8 ± 2.9	0.26 ± 0.02	8.5 ± 0.6
	2	96.8 ± 4.0	0.27 ± 0.02	6.0 ± 1.1
***T-2N*$_3$**	0	90.6 ± 0.9	0.15 ± 0.03	17.2 ± 0.8
	0.5	98.7 ± 1.3	0.15 ± 0.01	7.7 ± 0.6
	1	102.3 ± 2.1	0.19 ± 0.01	6.3 ± 1.0
	2	105.1 ± 1.9	0.17 ± 0.01	2.5 ± 0.3

3.4 Evaluation of pSar-shielding agents in vitro

Through the incorporation of pSar the unspecific interaction of polyplexes with cell membranes should be efficiently reduced as already demonstrated for other stealth-like polymers, e.g. PEG. To prove our assumption we performed uptake studies with pSar-shielded polyplexes. Polyplex formulations were prepared with Cy5-labled siRNA for this assay to follow the fluorescent cargo, incubated with neuroblastoma Neuro2a cells for 4 h at standard culture conditions and analyzed by flow cytometry. The signal intensity of cells labeled with fluorescent dye correlates with the amount of polyplexes being internalized (Table 2 and Figure S3). Unshielded material and material shielded with low equivalents of ***DBCO-PSar$_{119}$*** showed significant uptake into cells already after 4 h incubation time for both polyplex formulations prepared with one and two azide-bearing backbones (***T-1N$_3$*** and ***T-2N$_3$***). For ***T-1N$_3$*** formulations, a significant reduction in fluorescence intensity of more than 50% was observed for 1 eq of ***DBCO-PSar$_{119}$*** per oligomer, whereas 2 eq of ***DBCO-PSar$_{119}$*** were needed for ***T-2N$_3$*** formulations to reduce cell uptake (Table 2).

Table 2. Mean fluorescence intensity (MFI) for cellular internalization of Cy5-labeled siRNA formulations (left: ***T-1N$_3$***; right: ***T-2N$_3$***) shielded with increasing equivalents (eq mol/mol) of ***DBCO-PSar$_{119}$*** determined by flow cytometry.

siRNA formulation	eq DBCO-PSar$_{119}$	MFI	siRNA formulation	eq DBCO-PSar$_{119}$	MFI
T-1N$_3$	0	881.5 ± 25.5	***T-2N$_3$***	0	883.0 ± 86.0
	0.25	780.5 ± 2.5		0.25	870.5 ± 62.5
	0.5	715.0 ± 24.0		0.5	785.5 ± 38.5
	1	359.0 ± 14.0		1	602.5 ± 37.5
	2	245.5 ± 8.0		2	263.5 ± 4.5
untreated cells		2.4 ± 0.2			

The effect on internalization can be visualized by confocal laser scanning microscopy (CLSM). Cells were incubated with ***T-1N$_3$*** siRNA formulations for 4 h and the Cy5-labeled siRNA (red) representing the localization of the polyplex was detected (Figure 3). Compared to the unshielded material, which was avidly taken up by cells, 0.5 eq of ***DBCO-PSar$_{119}$*** showed a slight reduction in cellular internalization. For 1 eq of ***DBCO-PSar$_{119}$***, only a few polyplexes were taken up by cells, indicating a strong shielding ability. This experiment confirmed the observations made in the previously described flow cytometry studies.

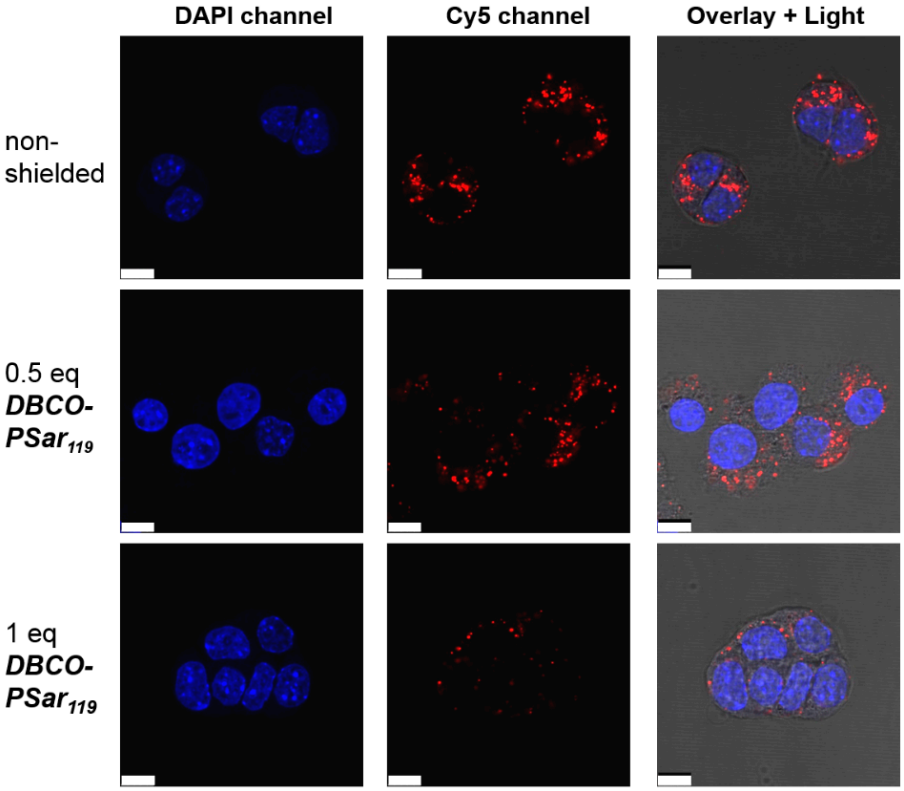

Figure 3. Intracellular distribution of ***T-1N₃*** siRNA formulations in Neuro2a-eGFP-Luc cells with increasing equivalents (eq mol/mol) of ***DBCO-PSar₁₁₉*** acquired by confocal laser scanning microscopy. Cells were incubated with the formulations for 4 h and washed with PBS buffer. Nuclei were stained with DAPI (blue) and siRNA was spiked with 20 % Cy5-labeled siRNA (red). The overlay image shows the merged channels and the light microscope image. Scale bar: 10 µm

In conclusion, covalent surface modification of polyplexes by SPAAC reduced cell binding and uptake substantially. Interestingly, the increase of azide functionalities in the ***T-2N₃*** backbone did not lead to a better surface passivation of the formed polyplex. As depicted in Table 2, both polyplexes behave comparably and differ only slightly at full polysarcosinylation levels. This observation may relate to differences in microstructure between ***T-1N₃*** and ***T-2N₃*** based polyplexes, which seems to influence the accessibility of azide on the polyplex surface.

3.5 Distribution of pSar- functionalized polyplexes in vivo

After the shielding ability of pSar-functionalized polyplexes could be demonstrated in biophysical and *in vitro* assays, we aim to explore the *in vivo* behavior of polysarcosinylated polyplexes. For *in vivo* biodistribution studies, the unshielded ***T-1N₃*** siRNA polyplex, which showed the lowest interaction with cells, was used to prepare a formulation to which either ***DBCO-PEG5k*** and a formulation using acetylated polysarcosine (***DBCO-PSar₁₁₉-Ac***; Figure 1, bottom) was covalently linked by SPAAC. The acetyl end group of ***DBCO-PSar₁₁₉-Ac*** seems to be better comparable to the commercial methoxylated PEG agent in terms of surface polarity. The cap of the *N*-terminal sarcosine slightly reduced migration distance of polyplexes in the gel in comparison to the non-acetylated pSar (Table S2, Figure S4). ***T-1N₃*** siRNA polyplexes were prepared with 50% Cy7-labeled siRNA and incubated with 1 eq of the respective shielding agent per oligomer for 4 h. A final concentration of 200 ng siRNA / µL was used for this experiment. 50 µg of siRNA and oligomers at an N/P ratio of 10 were used.

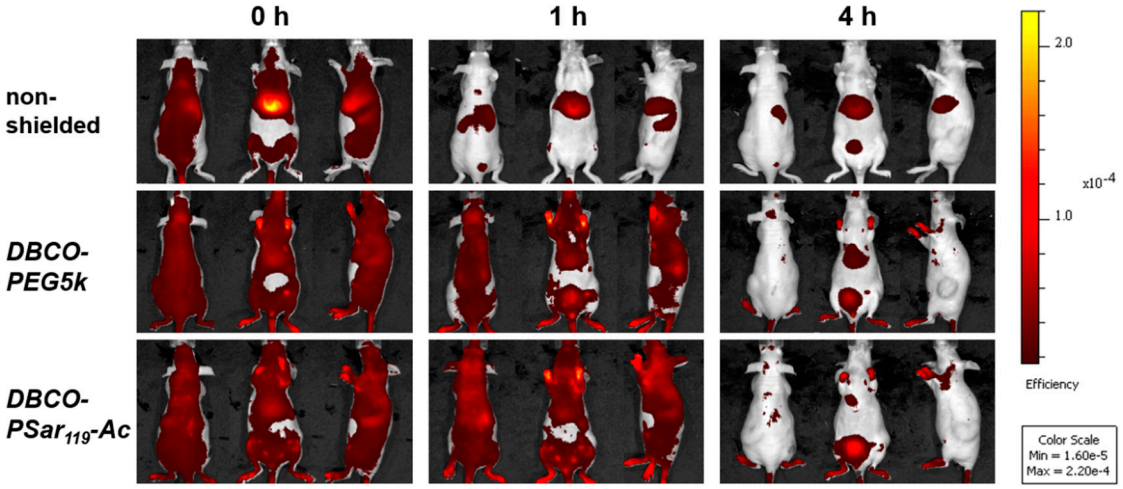

Figure 4. Biodistribution of ***T-1N₃*** siRNA formulations (50 µg siRNA; 50% Cy7-labeled) in NMRI-nude mice bearing Neuro2a tumors after *i.v.* administration. NIR fluorescence bioimages show formulations with 1 eq ***DBCO-PEG5k***, 1 eq acetylated ***DBCO-PSar₁₁₉-Ac*** or HBG buffer (non-shielded). Experiments were performed with two animals per group for time points until 60 min and one animal per group for later time points; a representative animal of each group is shown. Animals are presented in the dorsal, ventral and lateral view.

The formulations were injected into Neuro2a tumor-bearing mice via *i.v.* tail-vain injection and the distribution of the near infrared (NIR) fluorescent dye attached to the siRNA was monitored at various time points over 24h by bioimaging in mice (Figure 4, Figure S5). The unshielded polyplexes started accumulating in the liver after 15 min. Such a finding could also be observed for other unmodified T-shape backbone structures in previous work [89,90]. In contrast to the unshielded polyplexes, both shielded formulations showed much-extended circulation times and tumor accumulation. 60 minutes after injection of the material, the shielded formulations were still detectable in all areas of the body including the tumor site. After 4 h the intensity of the signals decreased, indicating a slow removal of polyplexes from circulation. The strongest signals remained in liver and bladder. In mice injected with shielded polyplexes, a strong signal was detected in the exposed periphery, such as the paws after more than 4 hours (Figure S5). In direct comparison, polyplexes with the ***DBCO-PSar₁₁₉-Ac*** and the ***DBCO-PEG5k*** displayed negligible differences in biodistribution, circulation time or tumor accumulation. A pronounced accumulation at the tumor site, however, could not be observed and may require further strategies to enhance tumor accessibility and retention.

3.6 Attachment of the targeting ligand folate to polysarcosine

The inhibition of unspecific cell binding is an important requirement for any specific interaction with cell surface receptors or proteins in solution. Thus, attaching a targeting ligand onto shielded polyplexes is expected to enable targeting of specific cell surface receptors. Since pSar offers the possibility to be further functionalized at its free secondary amino function, we chose folic acid (FolA) as a ligand to be conjugated to the *N*-terminus of ***DBCO-PSar₁₁₀*** by peptide bond formation. Folic acid is an interesting ligand, because it is a commercially available small molecule with carboxyl groups for conjugation and it is the natural ligand to the folic acid receptor (FR) overexpressed on several tumor types, e.g. prostate cancer [82-84,97-100]. The applied coupling conditions using equimolar amounts of folic acid, DBCO-PSar polymer and coupling reagents (2-(1*H*-benzotriazole-1-yl)-1,1,3,3-tetramethyluronium hexafluorophosphate (HBTU), 1-hydroxybenzotriazole (HOBt)) and the steric hindrance of the polymer avoid the formation of divalent folic acid conjugates. Concerning regioselectivity, it has been reported that both isoforms result for *N*,*N*-dicyclohexylcarbodiimide (DCC)-mediated amidation in DMSO or DMSO/DMF, but with an observed regioselectivity of 80% for the γ- conjugate (***DBCO-PSar₁₁₀-FolA***; Figure 1, Figure 5, Table S1) [101].

Preprints (www.preprints.org) | NOT PEER-REVIEWED | Posted: 29 May 2018 doi:10.20944/preprints201805.0423.v1

Peer-reviewed version available at Polymers 2018, 10, 689; doi:10.3390/polym10060689

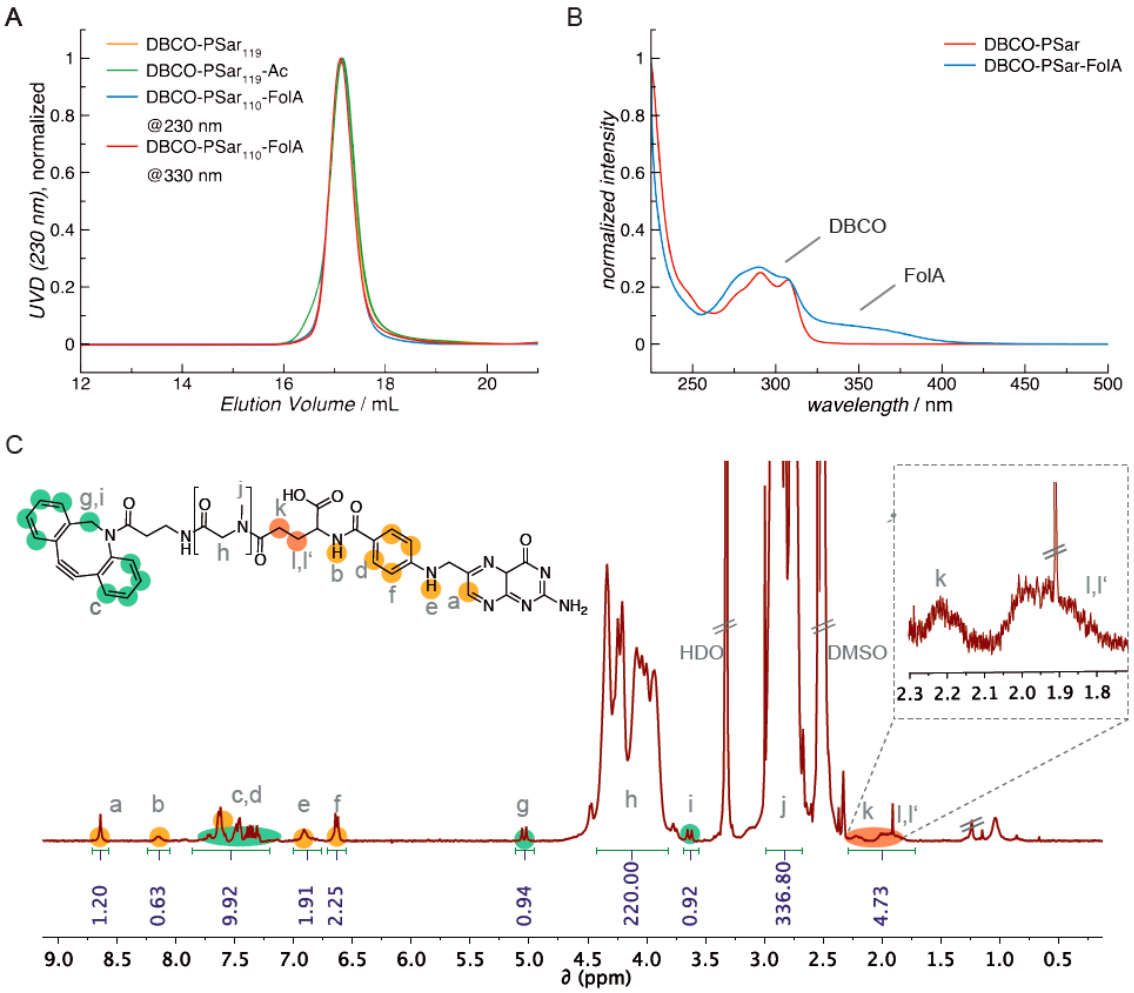

Figure 5. Characterization of DBCO-PSar ligands for post-shielding of polyplexes. A) GPC elugrams of DBCO-PSar in HFIP with different end groups. B) UV-vis spectrum of DBCO-PSar and DBCO-PSar-FolA, respectively. C) ^{1}H NMR spectrum of DBCOPSar-FolA in DMSO-*d6* (400 MHz).

The properties of ***T-1N***$_3$ siRNA polyplexes equipped with this negatively charged ligand changed in an unexpected way. For increasing equivalents, aggregates with high polydispersity were found by DLS (Table S1). An interesting finding was the change in size from around 80 to 25 nm of nanoparticles when folic acid was involved, which indicates strong compactation of the polyion complex. For small degrees of particle modification with ***DBCO-PSar***$_{110}$***-FolA***, the size of polyplexes did not significantly change compared to unshielded polyplexes. For higher amounts, aggregates were found in DLS measurements. Similar findings were observed for folic acid-targeted lipopolyplexes [102]. In the latter case, aggregation could be avoided by incorporation of tetra-glutamylated folic acid into the shielding agent. We observed that for further increase of ***DBCO-PSar***$_{110}$***-FolA*** to equimolar amounts, small defined particles of ~25 nm were found. This can only be explained with ***DBCO-PSar***$_{110}$***-FolA***-induced instability following a complete rearrangement of particles into a uniform population. The folic acid's chemical properties - its hydrophobic character and negative charge – seem to play a major role in this reassembly process, since it was not observed for untargeted polysarcosine-shielded particles.

When testing the folate targeted formulation with ***DBCO-PSar***$_{110}$***-FolA*** on a FR-overexpressing KB/eGFPLuc cell line, we found that targeted polyplexes showed increased binding to the cell surface, which could be blocked by folic acid competition (Figure S6A) ensuring FR mediated binding. Much to our surprise, the internalization of the polyplexes into the cell was extremely low (Figure S6A+B). As a consequence, no gene silencing activity was achieved with such systems (Figure S6C). Limitations in endosomal escape, often reported as being responsible for bad transfection

Peer-reviewed version available at Polymers 2018, 10, 689; doi:10.3390/polym10060689

efficiencies [103-107], can be excluded, since co-incubation with the lysosomotropic agent chloroquine did not improve gene silencing activity (Figure S6D). The trafficking of the vitamin folate via FR is reported to occur by a non-clathrin, non-caveolar pathway also known as CLIC/GEEC endocytosis pathway [104,108]. For folate-targeted nanoparticles however, it could be demonstrated that pathways like caveolae- and clathrin-mediated endocytosis occur [105,107,109]. The size and the ligand density on their surface were reported to influence the cellular uptake pathway. The well shielded, ~25 nm siRNA polyplexes do not seem to trigger any of the pathways in HeLa-derived KB cells efficiently. Further, the bioreducible carrier ***T-1N$_3$*** within the liopolyplex might be an easy prey for disulfide cleavage, which was reported to occur distinctly in the extracellular environment of HeLa cells [110]. The consequence of insufficient cellular uptake was a lack of gene silencing activity. This effect has been observed for folate-targeted polyplexes with 3.5 kDa PEG chains before [86]. At this point, we cannot provide an explanation for the observed findings and further studies need to be conducted to understand the fact that specific receptor binding was achieved, while receptor mediated endocytosis seems to be inhibited. In light of these *in vitro* data, a transfer of targeted polyplexes to *in vivo* studies was not performed based on ethical considerations.

4. Conclusions

To investigate the use of ability of pSar to shield polyplexes and enhance their circulation times and reduce unspecific interactions, we synthesized a polyplex formulation based on sequence defined lipo-oligomers and applied PEG and pSar based polymers for shielding of the preformed polyplexes. In previous work, a new class of redox-sensitive lipo-oligomers was successfully established for siRNA delivery. [39] For this reason, one of the best performing candidates from redox-sensitive lipo-oligomers was chosen and extended by a click-reactive azide functionality, resulting in carrier ***T-1N$_3$***. After the formation of siRNA lipopolyplexes, the particle surface was further modified with the shielding agent polysarcosine. The SPAAC could be performed between the DBCO-PSar polymer and the azide-containing lipo-oligomers within the polyplex. In addition, it was demonstrated that the grafting could be controlled stoichiometrically introducing a shielding layer. The shielding of the formed pSar corona has been observed *in vitro* in gel retardation assays and cell studies. In contrast to unmodified polyplexes, binding and cellular uptake was substantially reduced for all pSar-modified systems.

Furthermore, biodistribution in mice revealed that 8 kDa polysarcosine can strongly expand the circulation of the siRNA lipopolyplexes from several minutes to hours. The difference in non-shielded and shielded formulations is most pronounced at the 60 minutes time point, where in case of non-shielded polyplexes, most of the polyplexes have accumulated in the liver, but stable circulation is still observed for pSar-shielded polyplexes. While the biodistribution between non-modified polyplexes and polysarcosinylated systems differ substantially, such systems behaved similar to PEGylated polyplexes *in vivo*. Therefore, we can conclude that in terms of polyplex shielding pSar and PEG behave identically and can be both applied to reduce unspecific interactions of lipo-oligomer polyplexes and thus enhance blood circulation substantially from minutes to hours. When DBCO-PSar was, however, modified with folic acid to target cell surface receptors, not only the size of polyplexes was reduced from 80 to 25 nm, but also specific binding to FR-positive KB cell membranes did not boost cellular internalization. Therefore, we need to conclude that further investigations are necessary to combine favorable *in vivo* shielding with efficient receptor-targeted gene silencing for pSar-functionalized lipo-oligomer polyplexes.

Supplementary Materials: The following are available online, Figure S1: Synthesis of heterotelechelic DBCO-PSar polyplex shielding agents by NCA polymerization and subsequent amidation for further introduction of functionalities, Figure S2: siRNA binding ability of T-shape structures analyzed with an agarose gel shift assay, Figure S3: Cellular internalization of siRNA formulations shielded with increasing equivalents of ***DBCO-PSar$_{119}$*** determined by flow cytometry, Figure S4: Electrophoretic mobility of formulations, Figure S5: Biodistribution of siRNA formulations in NMRI-nude mice bearing Neuro2A tumors after *i.v.* administration, Figure S6: Cellular binding, cellular internalization and transfection efficiency of folate targeted siRNA polyplexes and untargeted

analogues, Table S1: Analytical data of synthesized heterotelechelic DBCO-PSar ligands, Table S2: Particle size and zeta potential of siRNA formulations determined with a DLS zetasizer.

Author Contributions: Philipp Klein performed chemistry of oligomers, preparation of the formulations and biophysical and cell-free *in vitro* experiments. Kristina Klinker synthesized and analyzed the DBCO agents. Wei Zhang performed transfections and FACS studies. Sarah Kern and Eva Kessel performed the *in vivo* experiment. Ernst Wagner and Matthias Barz supervised the experimental work and contributed with scientific discussions. Philipp Klein wrote the draft manuscript, Kristina Klinker, Matthias Barz and Ernst Wagner edited the manuscript, all other authors checked and contributed to the finalization of the manuscript.

Funding: This work was supported by German Research Foundation (DFG) CRC1066-1/-2 Projects A6, B5 and B12 as well as the Excellence Cluster Nanosystems Initiative Munich (NIM). KK would like to thank "Materials Science in Mainz" (MAINZ) and HaVo-foundation. WZ appreciates receiving a Bayerischen Gleichstellungsförderung fellowship as support for her postdoctoral research at LMU Munich.

Acknowledgments: We thank Miriam Höhn for generating the CLSM images.

Conflicts of Interest: The authors declare no conflict of interest.

References

1. Tabernero, J.; Shapiro, G.I.; LoRusso, P.M.; Cervantes, A.; Schwartz, G.K.; Weiss, G.J.; Paz-Ares, L.; Cho, D.C.; Infante, J.R.; Alsina, M., *et al.* First-in-humans trial of an rna interference therapeutic targeting vegf and ksp in cancer patients with liver involvement. *Cancer Discov* **2013**, *3*, 406-417, 10.1158/2159-8290.CD-12-0429.
2. Kacsinta, A.D.; Dowdy, S.F. Current views on inducing synthetic lethal rnai responses in the treatment of cancer. *Expert Opin Biol Ther* **2016**, *16*, 161-172, 10.1517/14712598.2016.1110141.
3. Haussecker, D. Current issues of rnai therapeutics delivery and development. *J Control Release* **2014**, *195*, 49-54, 10.1016/j.jconrel.2014.07.056.
4. Davis, M.E.; Zuckerman, J.E.; Choi, C.H.; Seligson, D.; Tolcher, A.; Alabi, C.A.; Yen, Y.; Heidel, J.D.; Ribas, A. Evidence of rnai in humans from systemically administered sirna via targeted nanoparticles. *Nature* **2010**, *464*, 1067-1070, 10.1038/nature08956.
5. Chou, S.T.; Mixson, A.J. Sirna nanoparticles: The future of rnai therapeutics for oncology? *Nanomedicine (Lond)* **2014**, *9*, 2251-2254, 10.2217/nnm.14.157.
6. Nair, J.K.; Willoughby, J.L.; Chan, A.; Charisse, K.; Alam, M.R.; Wang, Q.; Hoekstra, M.; Kandasamy, P.; Kel'in, A.V.; Milstein, S., *et al.* Multivalent n-acetylgalactosamine-conjugated sirna localizes in hepatocytes and elicits robust rnai-mediated gene silencing. *J Am Chem Soc* **2014**, *136*, 16958-16961, 10.1021/ja505986a.
7. Parmar, R.; Willoughby, J.L.; Liu, J.; Foster, D.J.; Brigham, B.; Theile, C.S.; Charisse, K.; Akinc, A.; Guidry, E.; Pei, Y., *et al.* 5'-(e)-vinylphosphonate: A stable phosphate mimic can improve the rnai activity of sirna-galnac conjugates. *Chembiochem* **2016**, *17*, 985-989, 10.1002/cbic.201600130.
8. Dohmen, C.; Edinger, D.; Frohlich, T.; Schreiner, L.; Lachelt, U.; Troiber, C.; Radler, J.; Hadwiger, P.; Vornlocher, H.P.; Wagner, E. Nanosized multifunctional polyplexes for receptor-mediated sirna delivery. *ACS Nano* **2012**, *6*, 5198-5208, 10.1021/nn300960m.
9. van de Water, F.M.; Boerman, O.C.; Wouterse, A.C.; Peters, J.G.; Russel, F.G.; Masereeuw, R. Intravenously administered short interfering rna accumulates in the kidney and selectively suppresses gene function in renal proximal tubules. *Drug Metab Dispos* **2006**, *34*, 1393-1397, 10.1124/dmd.106.009555.
10. Meade, B.R.; Gogoi, K.; Hamil, A.S.; Palm-Apergi, C.; van den Berg, A.; Hagopian, J.C.; Springer, A.D.; Eguchi, A.; Kacsinta, A.D.; Dowdy, C.F., *et al.* Efficient delivery of rnai prodrugs containing reversible charge-neutralizing phosphotriester backbone modifications. *Nat Biotechnol* **2014**, *32*, 1256-1261, 10.1038/nbt.3078.
11. Sakurai, Y.; Hatakeyama, H.; Sato, Y.; Hyodo, M.; Akita, H.; Harashima, H. Gene silencing via rnai and sirna quantification in tumor tissue using mend, a liposomal sirna delivery system. *Mol Ther* **2013**, *21*, 1195-1203, 10.1038/mt.2013.57.
12. Meyer, M.; Philipp, A.; Oskuee, R.; Schmidt, C.; Wagner, E. Breathing life into polycations: Functionalization with ph-responsive endosomolytic peptides and

polyethylene glycol enables sirna delivery. *Journal of the American Chemical Society* **2008**, *130*, 3272-+, 10.1021/ja710344v.

13. Meyer, M.; Dohmen, C.; Philipp, A.; Kiener, D.; Maiwald, G.; Scheu, C.; Ogris, M.; Wagner, E. Synthesis and biological evaluation of a bioresponsive and endosomolytic sirna-polymer conjugate. *Mol Pharm* **2009**, *6*, 752-762, 10.1021/mp9000124.
14. Wagner, E. Polymers for sirna delivery: Inspired by viruses to be targeted, dynamic, and precise. *Accounts of Chemical Research* **2012**, *45*, 1005-1013, 10.1021/ar2002232.
15. Wagner, E. Biomaterials in rnai therapeutics: Quo vadis? *Biomater Sci* **2013**, *1*, 804.
16. Pittella, F.; Cabral, H.; Maeda, Y.; Mi, P.; Watanabe, S.; Takemoto, H.; Kim, H.J.; Nishiyama, N.; Miyata, K.; Kataoka, K. Systemic sirna delivery to a spontaneous pancreatic tumor model in transgenic mice by pegylated calcium phosphate hybrid micelles. *J Control Release* **2014**, *178*, 18-24, 10.1016/j.jconrel.2014.01.008.
17. Lachelt, U.; Wagner, E. Nucleic acid therapeutics using polyplexes: A journey of 50 years (and beyond). *Chem Rev* **2015**, *115*, 11043-11078, 10.1021/cr5006793.
18. Leng, Q.; Chou, S.T.; Scaria, P.V.; Woodle, M.C.; Mixson, A.J. Increased tumor distribution and expression of histidine-rich plasmid polyplexes. *J Gene Med* **2014**, *16*, 317-328, 10.1002/jgm.2807.
19. Zintchenko, A.; Philipp, A.; Dehshahri, A.; Wagner, E. Simple modifications of branched pei lead to highly efficient sirna carriers with low toxicity. *Bioconjug Chem* **2008**, *19*, 1448-1455, 10.1021/bc800065f.
20. Whitehead, K.A.; Dorkin, J.R.; Vegas, A.J.; Chang, P.H.; Veiseh, O.; Matthews, J.; Fenton, O.S.; Zhang, Y.; Olejnik, K.T.; Yesilyurt, V.*, et al.* Degradable lipid nanoparticles with predictable in vivo sirna delivery activity. *Nat Commun* **2014**, *5*, 4277, 10.1038/ncomms5277.
21. Love, K.T.; Mahon, K.P.; Levins, C.G.; Whitehead, K.A.; Querbes, W.; Dorkin, J.R.; Qin, J.; Cantley, W.; Qin, L.L.; Racie, T.*, et al.* Lipid-like materials for low-dose, in vivo gene silencing. *Proc Natl Acad Sci U S A* **2010**, *107*, 1864-1869, 10.1073/pnas.0910603106.
22. Leng, Q.; Mixson, A.J. Small interfering rna targeting raf-1 inhibits tumor growth in vitro and in vivo. *Cancer Gene Ther* **2005**, *12*, 682-690, 10.1038/sj.cgt.7700831.
23. Miyata, K.; Nishiyama, N.; Kataoka, K. Rational design of smart supramolecular assemblies for gene delivery: Chemical challenges in the creation of artificial viruses. *Chem Soc Rev* **2012**, *41*, 2562-2574, 10.1039/c1cs15258k.
24. Kim, H.J.; Takemoto, H.; Yi, Y.; Zheng, M.; Maeda, Y.; Chaya, H.; Hayashi, K.; Mi, P.; Pittella, F.; Christie, R.J.*, et al.* Precise engineering of sirna delivery vehicles to tumors using polyion complexes and gold nanoparticles. *ACS Nano* **2014**, *8*, 8979-8991, 10.1021/nn502125h.
25. Li, S.D.; Chen, Y.C.; Hackett, M.J.; Huang, L. Tumor-targeted delivery of sirna by self-assembled nanoparticles. *Mol Ther* **2008**, *16*, 163-169, 10.1038/sj.mt.6300323.
26. Wang, X.L.; Ramusovic, S.; Nguyen, T.; Lu, Z.R. Novel polymerizable surfactants with ph-sensitive amphiphilicity and cell membrane disruption for efficient sirna delivery. *Bioconjug Chem* **2007**, *18*, 2169-2177, 10.1021/bc700285q.

27. Wang, X.L.; Xu, R.; Wu, X.; Gillespie, D.; Jensen, R.; Lu, Z.R. Targeted systemic delivery of a therapeutic sirna with a multifunctional carrier controls tumor proliferation in mice. *Mol Pharm* **2009**, *6*, 738-746, 10.1021/mp800192d.
28. Gujrati, M.; Vaidya, A.; Lu, Z.R. Multifunctional ph-sensitive amino lipids for sirna delivery. *Bioconjug Chem* **2016**, *27*, 19-35, 10.1021/acs.bioconjchem.5b00538.
29. Schafer, J.; Hobel, S.; Bakowsky, U.; Aigner, A. Liposome-polyethylenimine complexes for enhanced DNA and sirna delivery. *Biomaterials* **2010**, *31*, 6892-6900, 10.1016/j.biomaterials.2010.05.043.
30. Siegwart, D.J.; Whitehead, K.A.; Nuhn, L.; Sahay, G.; Cheng, H.; Jiang, S.; Ma, M.; Lytton-Jean, A.; Vegas, A.; Fenton, P., *et al.* Combinatorial synthesis of chemically diverse core-shell nanoparticles for intracellular delivery. *Proc Natl Acad Sci U S A* **2011**, *108*, 12996-13001, 10.1073/pnas.1106379108.
31. Green, J.J.; Langer, R.; Anderson, D.G. A combinatorial polymer library approach yields insight into nonviral gene delivery. *Acc Chem Res* **2008**, *41*, 749-759, 10.1021/ar7002336.
32. Uchida, H.; Miyata, K.; Oba, M.; Ishii, T.; Suma, T.; Itaka, K.; Nishiyama, N.; Kataoka, K. Odd-even effect of repeating aminoethylene units in the side chain of n-substituted polyaspartamides on gene transfection profiles. *J Am Chem Soc* **2011**, *133*, 15524-15532, 10.1021/ja204466y.
33. Frohlich, T.; Edinger, D.; Klager, R.; Troiber, C.; Salcher, E.; Badgujar, N.; Martin, I.; Schaffert, D.; Cengizeroglu, A.; Hadwiger, P., *et al.* Structure-activity relationships of sirna carriers based on sequence-defined oligo (ethane amino) amides. *J Control Release* **2012**, *160*, 532-541, 10.1016/j.jconrel.2012.03.018.
34. Krzyszton, R.; Salem, B.; Lee, D.J.; Schwake, G.; Wagner, E.; Radler, J.O. Microfluidic self-assembly of folate-targeted monomolecular sirna-lipid nanoparticles. *Nanoscale* **2017**, *9*, 7442-7453, 10.1039/c7nr01593c.
35. Leng, Q.; Scaria, P.; Zhu, J.; Ambulos, N.; Campbell, P.; Mixson, A.J. Highly branched hk peptides are effective carriers of sirna. *J Gene Med* **2005**, *7*, 977-986, 10.1002/jgm.748.
36. Gilleron, J.; Querbes, W.; Zeigerer, A.; Borodovsky, A.; Marsico, G.; Schubert, U.; Manygoats, K.; Seifert, S.; Andree, C.; Stoter, M., *et al.* Image-based analysis of lipid nanoparticle-mediated sirna delivery, intracellular trafficking and endosomal escape. *Nat Biotechnol* **2013**, *31*, 638-646, 10.1038/nbt.2612.
37. Sahay, G.; Querbes, W.; Alabi, C.; Eltoukhy, A.; Sarkar, S.; Zurenko, C.; Karagiannis, E.; Love, K.; Chen, D.; Zoncu, R., *et al.* Efficiency of sirna delivery by lipid nanoparticles is limited by endocytic recycling. *Nat Biotechnol* **2013**, *31*, 653-658, 10.1038/nbt.2614.
38. Wittrup, A.; Lieberman, J. Knocking down disease: A progress report on sirna therapeutics. *Nat Rev Genet* **2015**, *16*, 543-552, 10.1038/nrg3978.
39. Klein, P.M.; Reinhard, S.; Lee, D.J.; Muller, K.; Ponader, D.; Hartmann, L.; Wagner, E. Precise redox-sensitive cleavage sites for improved bioactivity of sirna lipopolyplexes. *Nanoscale* **2016**, *8*, 18098-18104, 10.1039/c6nr05767e.

40. Klibanov, A.L.; Maruyama, K.; Torchilin, V.P.; Huang, L. Amphipathic polyethyleneglycols effectively prolong the circulation time of liposomes. *FEBS Lett* **1990**, *268*, 235-237.
41. Senior, J.; Delgado, C.; Fisher, D.; Tilcock, C.; Gregoriadis, G. Influence of surface hydrophilicity of liposomes on their interaction with plasma protein and clearance from the circulation: Studies with poly (ethylene glycol)-coated vesicles. *Biochimica et Biophysica Acta (BBA)-Biomembranes* **1991**, *1062*, 77-82.
42. Mori, A.; Klibanov, A.L.; Torchilin, V.P.; Huang, L. Influence of the steric barrier activity of amphipathic poly (ethyleneglycol) and ganglioside gm1 on the circulation time of liposomes and on the target binding of immunoliposomes in vivo. *FEBS letters* **1991**, *284*, 263-266.
43. Yang, Q.; Lai, S.K. Anti-peg immunity: Emergence, characteristics, and unaddressed questions. *Wiley Interdiscip Rev Nanomed Nanobiotechnol* **2015**, *7*, 655-677, 10.1002/wnan.1339.
44. Plank, C.; Mechtler, K.; Szoka Jr, F.C.; Wagner, E. Activation of the complement system by synthetic DNA complexes: A potential barrier for intravenous gene delivery. *Human gene therapy* **1996**, *7*, 1437-1446.
45. Tockary, T.A.; Osada, K.; Motoda, Y.; Hiki, S.; Chen, Q.; Takeda, K.M.; Dirisala, A.; Osawa, S.; Kataoka, K. Rod-to-globule transition of pdna/peg–poly (l-lysine) polyplex micelles induced by a collapsed balance between DNA rigidity and peg crowdedness. *Small* **2016**, *12*, 1193-1200.
46. Merkel, O.M.; Librizzi, D.; Pfestroff, A.; Schurrat, T.; Buyens, K.; Sanders, N.N.; De Smedt, S.C.; Béhé, M.; Kissel, T. Stability of sirna polyplexes from poly (ethylenimine) and poly (ethylenimine)-g-poly (ethylene glycol) under in vivo conditions: Effects on pharmacokinetics and biodistribution measured by fluorescence fluctuation spectroscopy and single photon emission computed tomography (spect) imaging. *Journal of Controlled Release* **2009**, *138*, 148-159.
47. Kursa, M.; Walker, G.F.; Roessler, V.; Ogris, M.; Roedl, W.; Kircheis, R.; Wagner, E. Novel shielded transferrin− polyethylene glycol− polyethylenimine/DNA complexes for systemic tumor-targeted gene transfer. *Bioconjugate chemistry* **2003**, *14*, 222-231.
48. Fella, C.; Walker, G.F.; Ogris, M.; Wagner, E. Amine-reactive pyridylhydrazone-based peg reagents for ph-reversible pei polyplex shielding. *european journal of pharmaceutical sciences* **2008**, *34*, 309-320.
49. DeRouchey, J.; Walker, G.F.; Wagner, E.; Rädler, J.O. Decorated rods: A “bottom-up” self-assembly of monomolecular DNA complexes. *The Journal of Physical Chemistry B* **2006**, *110*, 4548-4554.
50. Moghimi, S.M.; Hunter, A.C.; Dadswell, C.M.; Savay, S.; Alving, C.R.; Szebeni, J. Causative factors behind poloxamer 188 (pluronic f68, flocor™)-induced complement activation in human sera: A protective role against poloxamer-mediated complement activation by elevated serum lipoprotein levels. *Biochimica et biophysica acta (BBA)-molecular basis of disease* **2004**, *1689*, 103-113.

51. Yang, Q.; Lai, S.K. Anti-peg immunity: Emergence, characteristics, and unaddressed questions. *Wiley Interdisciplinary Reviews: Nanomedicine and Nanobiotechnology* **2015**, *7*, 655-677.
52. Wenande, E.; Garvey, L. Immediate-type hypersensitivity to polyethylene glycols: A review. *Clinical & Experimental Allergy* **2016**, *46*, 907-922.
53. Knop, K.; Hoogenboom, R.; Fischer, D.; Schubert, U.S. Poly (ethylene glycol) in drug delivery: Pros and cons as well as potential alternatives. *Angewandte chemie international edition* **2010**, *49*, 6288-6308.
54. Hamad, I.; Hunter, A.; Szebeni, J.; Moghimi, S.M. Poly (ethylene glycol) s generate complement activation products in human serum through increased alternative pathway turnover and a masp-2-dependent process. *Molecular immunology* **2008**, *46*, 225-232.
55. Dewachter, P.; Mouton-Faivre, C. Anaphylaxis to macrogol 4000 after a parenteral corticoid injection. *Allergy* **2005**, *60*, 705-706.
56. Kircheis, R.; Wightman, L.; Schreiber, A.; Robitza, B.; Rössler, V.; Kursa, M.; Wagner, E. Polyethylenimine/DNA complexes shielded by transferrin target gene expression to tumors after systemic application. *Gene therapy* **2001**, *8*, 28.
57. Wang, W.; Tetley, L.; Uchegbu, I.F. The level of hydrophobic substitution and the molecular weight of amphiphilic poly-l-lysine-based polymers strongly affects their assembly into polymeric bilayer vesicles. *Journal of colloid and interface science* **2001**, *237*, 200-207.
58. Toncheva, V.; Wolfert, M.A.; Dash, P.R.; Oupicky, D.; Ulbrich, K.; Seymour, L.W.; Schacht, E.H. Novel vectors for gene delivery formed by self-assembly of DNA with poly (l-lysine) grafted with hydrophilic polymers. *Biochimica et Biophysica Acta (BBA)-General Subjects* **1998**, *1380*, 354-368.
59. Oupický, D.; Howard, K.A.; Koňák, Č.; Dash, P.R.; Ulbrich, K.; Seymour, L.W. Steric stabilization of poly-l-lysine/DNA complexes by the covalent attachment of semitelechelic poly [n-(2-hydroxypropyl) methacrylamide]. *Bioconjugate chemistry* **2000**, *11*, 492-501.
60. Lammers, T.; Ulbrich, K. Hpma copolymers: 30 years of advances. Elsevier: 2010.
61. Noga, M.; Edinger, D.; Kläger, R.; Wegner, S.V.; Spatz, J.P.; Wagner, E.; Winter, G.; Besheer, A. The effect of molar mass and degree of hydroxyethylation on the controlled shielding and deshielding of hydroxyethyl starch-coated polyplexes. *Biomaterials* **2013**, *34*, 2530-2538.
62. Li, C.; Wallace, S. Polymer-drug conjugates: Recent development in clinical oncology. *Adv Drug Deliv Rev* **2008**, *60*, 886-898, 10.1016/j.addr.2007.11.009.
63. Romberg, B.; Metselaar, J.M.; Baranyi, L.; Snel, C.J.; Bunger, R.; Hennink, W.E.; Szebeni, J.; Storm, G. Poly(amino acid)s: Promising enzymatically degradable stealth coatings for liposomes. *Int J Pharm* **2007**, *331*, 186-189, 10.1016/j.ijpharm.2006.11.018.
64. Schlapschy, M.; Binder, U.; Börger, C.; Theobald, I.; Wachinger, K.; Kisling, S.; Haller, D.; Skerra, A. Pasylation: A biological alternative to pegylation for extending

the plasma half-life of pharmaceutically active proteins. *Protein Engineering, Design & Selection* **2013**, *26*, 489-501.

65. Mendler, C.T.; Friedrich, L.; Laitinen, I.; Schlapschy, M.; Schwaiger, M.; Wester, H.-J.; Skerra, A. In *High contrast tumor imaging with radio-labeled antibody fab fragments tailored for optimized pharmacokinetics via pasylation*, MAbs, 2015; Taylor & Francis: pp 96-109.
66. Yoo, J.; Birke, A.; Kim, J.; Jang, Y.; Song, S.Y.; Ryu, S.; Kim, B.S.; Kim, B.G.; Barz, M.; Char, K. Cooperative catechol-functionalized polypept(o)ide brushes and ag nanoparticles for combination of protein resistance and antimicrobial activity on metal oxide surfaces. *Biomacromolecules* **2018**, *19*, 1602-1613, 10.1021/acs.biomac.8b00135.
67. Schneider, M.; Fetsch, C.; Amin, I.; Jordan, R.; Luxenhofer, R. Polypeptoid brushes by surface-initiated polymerization of n-substituted glycine n-carboxyanhydrides. *Langmuir* **2013**, *29*, 6983-6988, 10.1021/la4009174.
68. Schneider, M.; Tang, Z.; Richter, M.; Marschelke, C.; Forster, P.; Wegener, E.; Amin, I.; Zimmermann, H.; Scharnweber, D.; Braun, H.G.*, et al.* Patterned polypeptoid brushes. *Macromolecular Bioscience* **2016**, *16*, 75-81, 10.1002/mabi.201500314.
69. Birke, A.; Ling, J.; Barz, M. Polysarcosine-containing copolymers: Synthesis, characterization, self-assembly, and applications. *Progress in Polymer Science* **2018**, *81*, 163-208, 10.1016/j.progpolymsci.2018.01.002.
70. Fetsch, C.; Grossmann, A.; Holz, L.; Nawroth, J.F.; Luxenhofer, R. Polypeptoids from n-substituted glycine n-carboxyanhydrides: Hydrophilic, hydrophobic, and amphiphilic polymers with poisson distribution. *Macromolecules* **2011**, *44*, 6746-6758, 10.1021/ma201015y.
71. Klinker, K.; Barz, M. Polypept(o)ides: Hybrid systems based on polypeptides and polypeptoids. *Macromol Rapid Commun* **2015**, *36*, 1943-1957, 10.1002/marc.201500403.
72. Weber, B.; Birke, A.; Fischer, K.; Schmidt, M.; Barz, M. Solution properties of polysarcosine: From absolute and relative molar mass determinations to complement activation. *Macromolecules* **2018**, *51*, 2653-2661, 10.1021/acs.macromol.8b00258.
73. Wei, Q.; Becherer, T.; Angioletti-Uberti, S.; Dzubiella, J.; Wischke, C.; Neffe, A.T.; Lendlein, A.; Ballauff, M.; Haag, R. Protein interactions with polymer coatings and biomaterials. *Angew Chem Int Ed Engl* **2014**, *53*, 8004-8031, 10.1002/anie.201400546.
74. Hörtz, C.; Birke, A.; Kaps, L.; Decker, S.; Wächtersbach, E.; Fischer, K.; Schuppan, D.; Barz, M.; Schmidt, M. Cylindrical brush polymers with polysarcosine side chains: A novel biocompatible carrier for biomedical applications. *Macromolecules* **2015**, *48*, 2074-2086, 10.1021/ma502497x.
75. Sela, M. Immunological studies with synthetic polypeptides. *Adv Immunol* **1966**, *5*, 29-129.
76. Hara, E.; Ueda, M.; Kim, C.J.; Makino, A.; Hara, I.; Ozeki, E.; Kimura, S. Suppressive immune response of poly-(sarcosine) chains in peptide-nanosheets in contrast to polymeric micelles. *J Pept Sci* **2014**, *20*, 570-577, 10.1002/psc.2655.

77. Birke, A.; Huesmann, D.; Kelsch, A.; Weilbacher, M.; Xie, J.; Bros, M.; Bopp, T.; Becker, C.; Landfester, K.; Barz, M. Polypeptoid-block-polypeptide copolymers: Synthesis, characterization, and application of amphiphilic block copolypept(o)ides in drug formulations and miniemulsion techniques. *Biomacromolecules* **2014**, *15*, 548-557, 10.1021/bm401542z.

78. Otter, R.; Klinker, K.; Spitzer, D.; Schinnerer, M.; Barz, M.; Besenius, P. Folding induced supramolecular assembly into ph-responsive nanorods with a protein repellent shell. *Chem Commun* **2018**, *54*, 401-404, 10.1039/c7cc08127h.

79. Heller, P.; Hobernik, D.; Lachelt, U.; Schinnerer, M.; Weber, B.; Schmidt, M.; Wagner, E.; Bros, M.; Barz, M. Combining reactive triblock copolymers with functional cross-linkers: A versatile pathway to disulfide stabilized-polyplex libraries and their application as pdna vaccines. *Journal of Controlled Release* **2017**, *258*, 146-160, 10.1016/j.jconrel.2017.05.012.

80. Klinker, K.; Schafer, O.; Huesmann, D.; Bauer, T.; Capeloa, L.; Braun, L.; Stergiou, N.; Schinnerer, M.; Dirisala, A.; Miyata, K.*, et al.* Secondary-structure-driven self-assembly of reactive polypept(o)ides: Controlling size, shape, and function of core cross-linked nanostructures. *Angew Chem Int Ed Engl* **2017**, *56*, 9608-9613, 10.1002/anie.201702624.

81. Duro-Castano, A.; Movellan, J.; Vicent, M.J. Smart branched polymer drug conjugates as nano-sized drug delivery systems. *Biomater Sci* **2015**, *3*, 1321-1334, 10.1039/c5bm00166h.

82. Park, E.K.; Kim, S.Y.; Lee, S.B.; Lee, Y.M. Folate-conjugated methoxy poly(ethylene glycol)/poly(epsilon-caprolactone) amphiphilic block copolymeric micelles for tumor-targeted drug delivery. *J Control Release* **2005**, *109*, 158-168, 10.1016/j.jconrel.2005.09.039.

83. Xia, W.; Low, P.S. Folate-targeted therapies for cancer. *J Med Chem* **2010**, *53*, 6811-6824, 10.1021/jm100509v.

84. Sudimack, J.; Lee, R.J. Targeted drug delivery via the folate receptor. *Adv Drug Deliv Rev* **2000**, *41*, 147-162.

85. Low, P.S.; Henne, W.A.; Doorneweerd, D.D. Discovery and development of folic-acid-based receptor targeting for imaging and therapy of cancer and inflammatory diseases. *Acc Chem Res* **2008**, *41*, 120-129, 10.1021/ar7000815.

86. Klein, P.M.; Kern, S.; Lee, D.J.; Schmaus, J.; Hohn, M.; Gorges, J.; Kazmaier, U.; Wagner, E. Folate receptor-directed orthogonal click-functionalization of sirna lipopolyplexes for tumor cell killing in vivo. *Biomaterials* **2018**, 10.1016/j.biomaterials.2018.03.031.

87. Shi, B.; Keough, E.; Matter, A.; Leander, K.; Young, S.; Carlini, E.; Sachs, A.B.; Tao, W.; Abrams, M.; Howell, B.*, et al.* Biodistribution of small interfering rna at the organ and cellular levels after lipid nanoparticle-mediated delivery. *J Histochem Cytochem* **2011**, *59*, 727-740, 10.1369/0022155411410885.

88. Akinc, A.; Querbes, W.; De, S.; Qin, J.; Frank-Kamenetsky, M.; Jayaprakash, K.N.; Jayaraman, M.; Rajeev, K.G.; Cantley, W.L.; Dorkin, J.R.*, et al.* Targeted delivery of

rnai therapeutics with endogenous and exogenous ligand-based mechanisms. *Mol Ther* **2010**, *18*, 1357-1364, 10.1038/mt.2010.85.

89. Zhang, W.; Muller, K.; Kessel, E.; Reinhard, S.; He, D.; Klein, P.M.; Hohn, M.; Rodl, W.; Kempter, S.; Wagner, E. Targeted sirna delivery using a lipo-oligoaminoamide nanocore with an influenza peptide and transferrin shell. *Adv Healthc Mater* **2016**, *5*, 1493-1504, 10.1002/adhm.201600057.

90. Troiber, C.; Edinger, D.; Kos, P.; Schreiner, L.; Klager, R.; Herrmann, A.; Wagner, E. Stabilizing effect of tyrosine trimers on pdna and sirna polyplexes. *Biomaterials* **2013**, *34*, 1624-1633, 10.1016/j.biomaterials.2012.11.021.

91. Schottler, S.; Becker, G.; Winzen, S.; Steinbach, T.; Mohr, K.; Landfester, K.; Mailander, V.; Wurm, F.R. Protein adsorption is required for stealth effect of poly(ethylene glycol)- and poly(phosphoester)-coated nanocarriers. *Nat Nanotechnol* **2016**, *11*, 372-377, 10.1038/nnano.2015.330.

92. Pozzi, D.; Caracciolo, G.; Marchini, C.; Montani, M.; Amici, A.; Callipo, L.; Capriotti, A.L.; Cavaliere, C.; Lagana, A. Surface adsorption of protein corona controls the cell uptake mechanism in efficient cationic liposome/DNA complexes in serum. *J Control Release* **2010**, *148*, e94-95, 10.1016/j.jconrel.2010.07.069.

93. Lundqvist, M.; Stigler, J.; Elia, G.; Lynch, I.; Cedervall, T.; Dawson, K.A. Nanoparticle size and surface properties determine the protein corona with possible implications for biological impacts. *Proc Natl Acad Sci U S A* **2008**, *105*, 14265-14270, 10.1073/pnas.0805135105.

94. Fokina, A.; Klinker, K.; Braun, L.; Jeong, B.G.; Bae, W.K.; Barz, M.; Zentel, R. Multidentate polysarcosine-based ligands for water-soluble quantum dots. *Macromolecules* **2016**, *49*, 3663-3671, 10.1021/acs.macromol.6b00582.

95. Klinker, K.; Holm, R.; Heller, P.; Barz, M. Evaluating chemical ligation techniques for the synthesis of block copolypeptides, polypeptoids and block copolypept(o)ides: A comparative study. *Polym Chem-Uk* **2015**, *6*, 4612-4623, 10.1039/c5py00461f.

96. Dommerholt, J.; Rutjes, F.; van Delft, F.L. Strain-promoted 1,3-dipolar cycloaddition of cycloalkynes and organic azides. *Top Curr Chem (Cham)* **2016**, *374*, 16, 10.1007/s41061-016-0016-4.

97. Lee, D.J.; Kessel, E.; Lehto, T.; Liu, X.; Yoshinaga, N.; Padari, K.; Chen, Y.C.; Kempter, S.; Uchida, S.; Radler, J.O., *et al.* Systemic delivery of folate-peg sirna lipopolyplexes with enhanced intracellular stability for in vivo gene silencing in leukemia. *Bioconjug Chem* **2017**, *28*, 2393-2409, 10.1021/acs.bioconjchem.7b00383.

98. Dohmen, C.; Frohlich, T.; Lachelt, U.; Rohl, I.; Vornlocher, H.P.; Hadwiger, P.; Wagner, E. Defined folate-peg-sirna conjugates for receptor-specific gene silencing. *Mol Ther Nucleic Acids* **2012**, *1*, e7, 10.1038/mtna.2011.10.

99. Leamon, C.P.; Low, P.S. Folate-mediated targeting: From diagnostics to drug and gene delivery. *Drug Discov Today* **2001**, *6*, 44-51.

100. Leamon, C.P.; DePrince, R.B.; Hendren, R.W. Folate-mediated drug delivery: Effect of alternative conjugation chemistry. *J Drug Target* **1999**, *7*, 157-169, 10.3109/10611869909085499.

101. Wang, S.; Lee, R.J.; Mathias, C.J.; Green, M.A.; Low, P.S. Synthesis, purification, and tumor cell uptake of 67ga-deferoxamine--folate, a potential radiopharmaceutical for tumor imaging. *Bioconjug Chem* **1996**, *7*, 56-62, 10.1021/bc9500709.

102. Muller, K.; Kessel, E.; Klein, P.M.; Hohn, M.; Wagner, E. Post-pegylation of sirna lipo-oligoamino amide polyplexes using tetra-glutamylated folic acid as ligand for receptor-targeted delivery. *Mol Pharm* **2016**, *13*, 2332-2345, 10.1021/acs.molpharmaceut.6b00102.

103. Nie, Y.; Gunther, M.; Gu, Z.; Wagner, E. Pyridylhydrazone-based pegylation for ph-reversible lipopolyplex shielding. *Biomaterials* **2011**, *32*, 858-869, 10.1016/j.biomaterials.2010.09.032.

104. Maldonado-Baez, L.; Williamson, C.; Donaldson, J.G. Clathrin-independent endocytosis: A cargo-centric view. *Exp Cell Res* **2013**, *319*, 2759-2769, 10.1016/j.yexcr.2013.08.008.

105. Li, Y.L.; Van Cuong, N.; Hsieh, M.F. Endocytosis pathways of the folate tethered star-shaped peg-pcl micelles in cancer cell lines. *Polymers-Basel* **2014**, *6*, 634-650, 10.3390/polym6030634.

106. Langston Suen, W.L.; Chau, Y. Size-dependent internalisation of folate-decorated nanoparticles via the pathways of clathrin and caveolae-mediated endocytosis in arpe-19 cells. *J Pharm Pharmacol* **2014**, *66*, 564-573, 10.1111/jphp.12134.

107. Dalal, C.; Saha, A.; Jana, N.R. Nanoparticle multivalency directed shifting of cellular uptake mechanism. *J Phys Chem C* **2016**, *120*, 6778-6786, 10.1021/acs.jpcc.5b11059.

108. Sabharanjak, S.; Sharma, P.; Parton, R.G.; Mayor, S. Gpi-anchored proteins are delivered to recycling endosomes via a distinct cdc42-regulated, clathrin-independent pinocytic pathway. *Dev Cell* **2002**, *2*, 411-423.

109. Suen, W.L.L.; Chau, Y. Size- dependent internalisation of folate- decorated nanoparticles via the pathways of clathrin and caveolae- mediated endocytosis in arpe-19 cells. *J Pharm Pharmacol* **2014**, *66*, 564-573, 10.1111/jphp.12134.

110. Brulisauer, L.; Kathriner, N.; Prenrecaj, M.; Gauthier, M.A.; Leroux, J.C. Tracking the bioreduction of disulfide-containing cationic dendrimers. *Angew Chem Int Ed Engl* **2012**, *51*, 12454-12458, 10.1002/anie.201207070.